Inorganic Chemistry

Article

pubs.acs.org/IC

# First Palladium(II) and Platinum(II) Complexes from Employment of 2,6-Diacetylpyridine Dioxime: Synthesis, Structural and Spectroscopic Characterization, and Biological Evaluation

Evangelia S. Koumousi,[†] Marianthi Zampakou,[∥] Catherine P. Raptopoulou,[‡] Vassilis Psycharis,[‡] Christine M. Beavers,[§] Simon J. Teat,[§] George Psomas,*[,∥] and Theocharis C. Stamatatos*[,†,∥]

[†]Department of Chemistry, University of Patras, GR-265 04 Patras, Greece

[‡]Institute of Materials Science, NCSR "Demokritos", GR-153 10 Aghia Paraskevi Attikis, Greece

[§]Advanced Light Source, Lawrence Berkeley National Laboratory, 1 Cyclotron Road, Mail Stop 2-400, Berkeley, California 94720, United States

[∥]Department of General and Inorganic Chemistry, Faculty of Chemistry, Aristotle University of Thessaloniki, P.O. Box 135, GR-54124 Thessaloniki, Greece

Supporting Information

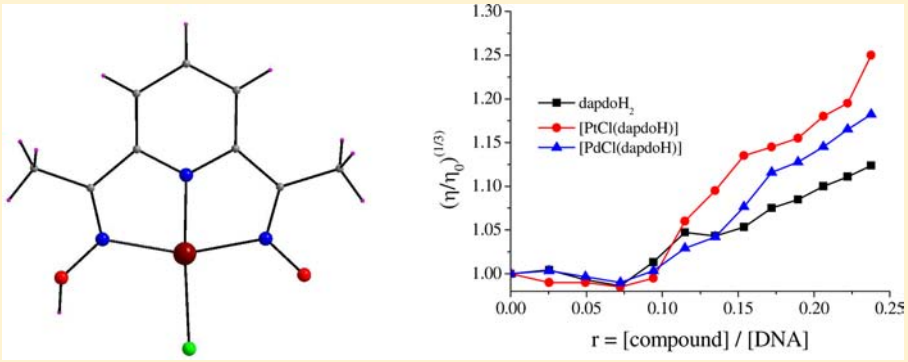


**ABSTRACT:** Employment of the monoanion of 2,6-diacetylpyridine dioxime ($dapdoH_2$) as a tridentate chelate in palladium(II) and platinum(II) chemistry is reported. The syntheses, crystal structures, spectroscopic and physicochemical characterization, and biological evaluation are described of [PdCl(dapdoH)] (**1**) and [PtCl(dapdoH)] (**2**). Reaction of $PdCl_2$ with 2 equivs of $dapdoH_2$ in MeOH under reflux gave **1**, whereas the same reaction with $PtCl_2$ in place of $PdCl_2$ gave **2** in comparable yields (70−80%). The divalent metal center in both compounds is coordinated by a terminal chloro group and a *N*,*N*′,*N*″-tridentate chelating ($\eta^3$) $dapdoH^-$ ligand. Thus, each metal ion is four coordinate with a distorted square planar geometry. Characterization of both complexes with $^1H$ and $^{13}C$ NMR and UV−vis and electrospray ionization mass spectroscopies confirmed their integrity in DMSO solutions. Interaction of the complexes with human and bovine serum albumin has been studied with fluorescence spectroscopy, revealing their affinity for these proteins with relatively high values of binding constants. UV study of the interaction of the complexes with calf-thymus DNA (CT DNA) has shown that they can bind to CT DNA, and the corresponding DNA binding constants have been evaluated. Cyclic voltammograms of the complexes in the presence of CT DNA solution have shown that the interaction of the complexes with CT DNA is mainly through intercalation, which has been also shown by DNA solution viscosity measurements. Competitive studies with ethidium bromide (EB) have revealed the ability of the complexes to displace the DNA-bound EB, suggesting competition with EB. The combined work demonstrates the ability of pyridyl−dioxime chelates not only to lead to polynuclear 3d-metal complexes with impressive structural motifs and interesting magnetic properties but also to yield new, mononuclear 4d- and 5d-metal complexes with biological implications.

## INTRODUCTION

Pyridyl oximes and dioximes with general formula (py){C(R)-NOH}$_x$ [R = various; $x$ = 1 (for monoximes) or 2 (for dioximes); Figure 1, top] constitute a very important class of compounds related to biological systems. The strong nucleophilicity of the oximate anion, >C═N−O$^-$, is associated with many hydrolytic processes, such as transfer or cleavage of an acyl, a phosphoryl, or a sulfuryl group, by attacking an electrophilic center.[1] Among these actions, the fact that a family of pyridyl oximes has shown a pronounced ability to reactivate the enzyme acetylcholinesterase (AChE), when it is fully inhibited by organophosphorus compounds (OPs), including pesticides and chemical warfare agents, is of particular

**Received:** April 10, 2012
**Published:** June 28, 2012

   dx.doi.org/10.1021/ic300739x | *Inorg. Chem.* 2012, 51, 7699−7710

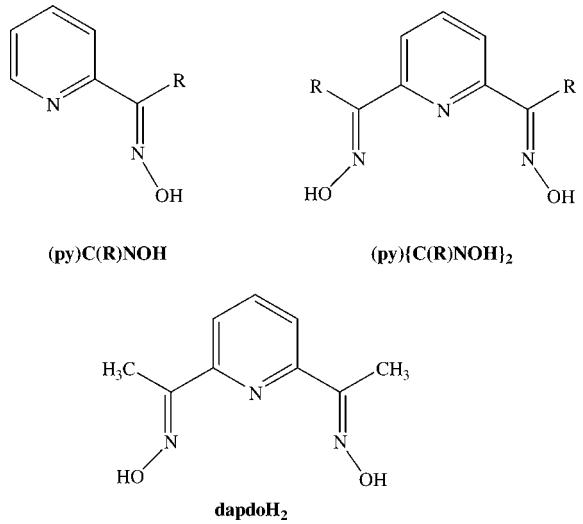


**Figure 1.** General structural formulas and abbreviations of the pyridyl monoximes [(py)C(R)NOH] and dioximes [(py){C(R)NOH}$_2$] discussed in the text (top) and ligand 2,6-diacetylpyridine dioxime (dapdoH$_2$; R− = $CH_3$−) employed in the present work (bottom).

pharmaceutical interest.[2−5] Further, a wide spectrum of biological activity of derivatives of pyridyl oximes has been investigated, such as activity on the cardiovascular system, as a sedative, antidepressant and antispasmodic activity, analgesic and anti-inflammatory activity, among others.[6]

On the other hand, there is currently renewed interest in the coordination chemistry of pyridyl oximes and dioximes whose anions are versatile ligands for a variety of objectives, including bridging affinity and formation of polynuclear metal complexes (clusters), isolation of coordination polymers, mixed-metal chemistry, and significant magnetic characteristic.[7,8] From a bioinorganic point of view, complexation of a metal ion with a pyridyloximate ligand would help the nucleophilicity of the oximate anion by lowering the p$K$ of the molecule to an extent near physiological values.[9,10] It is furthermore known that metal complexes of biologically active compounds possess features of considerable pharmaceutical interest because of several factors. In fact, the field of medicinal inorganic chemistry emerged a long time ago,[11] and it is based on certain principles such as (a) complexation with the metal protects the drug against enzymatic degradation because of the inertness of certain metal−ligand linkages, (b) the metal complex can have better hydrophobicity/hydrophilicity properties than the free ligand and through this can improve the transport processes in the tissues, (c) the metal complex can release the active drug(s) in a specific organ, and its activity can be reinforced by the combination of effects from the ligands and from the metal residue. Worldwide research based on these principles is focused on the design of metal-based drugs.[12]

The majority of synthetic metal complexes used as antitumor chemotherapeutic compounds are structural analogues of the neutral cisplatin, *cis*-[Pt$^{II}$Cl$_2$(NH$_3$)$_2$].[13] Many platinum(II) complexes that are *trans* in geometry[14] or charged[15] have been found to be also active. Recently, increasing interest has been shown to "rule breakers" in the hope of finding new candidates that could interact differently with biological targets as compared to that of cisplatin.[16] A number of these complexes have exhibited biological profiles distinctly different than those of cisplatin and its analogues.[17−19] In addition to the prolonged biological interest in platinum(II) complexes, palladium(II) analogues were recently included among the newly introduced structural types of metal complexes, designed for increased antitumor efficiency and decreased toxicity to normal cells.[20] The first of these had little or no application as antitumor compounds, due to the poor stability and rapid hydrolysis in biological environments. However, employment of chelating ligands in their synthesis was essential for improvement of their stability, which was further increased by generation of cyclopalladated compounds.[21]

Given the essential pharmaceutical and biological use of Pd$^{II}$ and Pt$^{II}$ complexes and the broad biological activity of pyridyl oximes and dioximes, it is rather surprising that the coordination chemistry of these metal ions with various pyridyl dioximes is completely unexplored. On the basis of this observation and our previous experience with employment of pyridyl dioxime ligands in 3d-metal cluster chemistry,[8b,d] we recently started a program aiming at systematic investigation of the M$^{II}$/pyridyl dioxime system (M = Pd, Pt) by means of exploring the structural and chemical characteristics of the new complexes, study of their physicochemical properties, and evaluation of their biological activity.

Toward this end, we herein report our first results from employment of 2,6-diacetylpyridine dioxime (dapdoH$_2$; Figure 1, bottom) ligand in Pd$^{II}$ and Pt$^{II}$ chemistry, which has produced the new compounds [PdCl(dapdoH)] (**1**) and [PtCl(dapdoH)] (**2**). The synthesis, structures, physicochemical characterization, and biological implication of the products are described in this work.

## EXPERIMENTAL SECTION

**Syntheses.** All manipulations were performed under aerobic conditions using chemicals and solvents as received, unless otherwise stated. Specifically, trisodium citrate, NaCl, calf-thymus (CT DNA), bovine serum albumin (BSA), human serum albumin (HSA), and ethidium bromide (EB) were purchased from Sigma-Aldrich Co, and all solvents relevant to the physicochemical and biological characterization were purchased from Merck. The organic ligand dapdoH$_2$ was synthesized as previously reported.[22] The ligand is soluble in DMSO, and its UV−vis spectra ($\lambda$/nm; $\varepsilon$/M$^{-1}$ cm$^{-1}$) have been recorded as a Nujol mull (295 nm) and in DMSO solution (293 nm; 10 500 M$^{-1}$ cm$^{-1}$).

DNA stock solution was prepared by dilution of CT DNA to buffer (containing 150 mM NaCl and 15 mM trisodium citrate at pH 7.0) followed by exhaustive stirring at 4 °C for 3 days and kept at 4 °C for no longer than 1 week. The stock solution of CT DNA gave a ratio of UV absorbance at 260 and 280 nm ($A_{260}/A_{280}$) of 1.89, indicating that the DNA was sufficiently free of protein contamination. The DNA concentration was determined by the UV absorbance at 260 nm after 1:20 dilution using $\varepsilon$ = 6600 M$^{-1}$ cm$^{-1}$.[23]

**[PdCl(dapdoH)] (1).** To a stirred colorless solution of dapdoH$_2$ (0.12 g, 0.60 mmol) in MeOH (30 mL) was added solid PdCl$_2$ (0.05 g, 0.30 mmol). The resulting yellow slurry was refluxed for 5 h, during which time the entire PdCl$_2$ solid dissolved and the color of the solution turned to orange. The latter solution was then allowed to slowly concentrate by solvent evaporation at room temperature for a period of 4−5 days. Well-formed orange needle-shaped crystals of **1** appeared and were collected by filtration, washed with cold MeOH (2 × 3 mL) and Et$_2$O (2 × 5 mL), and dried in air; the yield was 0.07 g (~70% based on Pd). Anal. Calcd for **1**: C, 32.36; H, 3.02; N, 12.58. Found: C, 32.52; H, 3.19; N, 12.44. Selected IR data (cm$^{-1}$): 3442 (mb), 3058 (m), 3028 (m), 2914 (w), 1574 (m), 1478 (m), 1454 (s), 1388 (vs), 1348 (m), 1280 (m), 1238 (vs), 1184 (vs), 1154 (vs), 1094 (s), 1058 (vs), 1038 (s), 914 (m), 850 (w), 800 (s), 732 (m), 708 (s), 554 (w), 512 (w), 488 (s), 418 (s). UV−vis, $\lambda$/nm ($\varepsilon$/M$^{-1}$ cm$^{-1}$) as Nujol mull: 570 (sh), 520 (sh), 402 (sh), 333 (sh), 305. UV−vis, $\lambda$/nm ($\varepsilon$/M$^{-1}$ cm$^{-1}$) in DMSO: 563 (150), 520 (sh) (120), 395 (sh)


dx.doi.org/10.1021/ic300739x | Inorg. Chem. 2012, 51, 7699−7710

(850), 338 (5200), 300 (13300). The complex is soluble in DMSO ($\Lambda_M$ = 7 mho cm$^2$ mol$^{-1}$, in 1 mM DMSO solution).

**[PtCl(dapdoH)] (2).** To a stirred colorless solution of dapdoH$_2$ (0.12 g, 0.60 mmol) in MeOH (30 mL) was added solid PtCl$_2$ (0.08 g, 0.30 mmol). The resulting brownish slurry was refluxed for 5 h, during which time the entire PtCl$_2$ solid dissolved and the color of the solution turned to dark red. The latter solution was then allowed to slowly concentrate by solvent evaporation at room temperature for a period of 3−4 days. Well-formed red plate-like crystals of **2** appeared and were collected by filtration, washed with cold MeOH (2 × 3 mL) and Et$_2$O (2 × 5 mL), and dried in air; the yield was 0.10 g (∼80% based on Pt). Anal. Calcd for **2**: C, 25.57; H, 2.38; N, 9.94. Found: C, 25.71; H, 2.45; N, 9.78. Selected IR data (cm$^{-1}$): 3448 (mb), 3062 (m), 3025 (m), 2916 (w), 1590 (m), 1478 (m), 1444 (s), 1388 (vs), 1342 (m), 1282 (m), 1234 (m), 1156 (s), 1096 (m), 1068 (vs), 1036 (s), 912 (w), 856 (w), 796 (s), 734 (m), 710 (m), 686 (w), 558 (w), 522 (w), 500 (m), 422 (m). UV−vis, $\lambda$/nm ($\varepsilon$/M$^{-1}$ cm$^{-1}$) as Nujol mull: 580 (sh), 530 (sh), 390 (sh), 336, 301. UV−vis, $\lambda$/nm ($\varepsilon$/M$^{-1}$ cm$^{-1}$) in DMSO: 575 (sh) (40), 539 (sh) (400), 391 (sh) (1750), 335 (9100), 297 (9500). The complex is soluble in DMSO ($\Lambda_M$ = 12 mho cm$^2$ mol$^{-1}$, in 1 mM DMSO solution).

**Single-Crystal X-ray Crystallography.** Data for a selected crystal of **1** were collected at Station 11.3.1 of the Advanced Light Source at Lawrence Berkeley National Laboratory using a Bruker Apex II CCD diffractometer ($\omega_o$ rotation with narrow frames, synchrotron radiation at 0.77490 Å, Silicon 111 monochromator). The structure was solved by direct methods and refined using the SHELX-TL suite.[24] All non-H atoms were refined anisotropically. H atoms were placed in geometrically suitable positions where possible, whereas the methyl and hydroxyl H atoms were found in the difference map and constrained using a riding model.

Data for a selected crystal of **2** were collected on a Rigaku R-AXIS SPIDER Image Plate diffractometer using graphite-monochromated Cu K$\alpha$ radiation ($\lambda$ = 1.54178 Å). Unit cell dimensions were determined and refined using the angular settings of 25 automatically centered reflections in the range 11° < 2$\theta$ < 23°. Intensity data were recorded using a $\theta$−2$\theta$ scan to a maximum 2$\theta$ value of 130°. Three standard reflections monitored every 97 reflections showed less than 3% variation and no decay. Lorentz, polarization, and psi-scan absorption corrections were applied using CrystalClear software.[25] The structure was solved by direct methods using SHELXS-97[26a] and refined on $F^2$ by full-matrix least-squares techniques with SHELXL-97.[26b] All H atoms were either located by Fourier difference maps and refined isotropically or introduced at calculated positions as riding on bonded atoms. All non-H atoms were refined anisotropically. The programs used for molecular graphics were MERCURY[27] and DIAMOND.[28]

Unit cell parameters and structure solution and refinement data for the two complexes are listed in Table 1.

**Physical Measurements.** Infrared (IR) spectra were recorded in the solid state (KBr pellets) on a Perkin-Elmer 16 PC FT spectrometer in the 4000−400 cm$^{-1}$ range. Far-IR spectra (500−100 cm$^{-1}$) were recorded on a Bruker IFS 113v FT spectrometer with a DTGS detector using polyethylene pellets. Elemental analyses (C, H, and N) were performed by the in-house facilities of the University of Patras using an EA 1108 Carlo Erba analyzer. $^1$H and $^{13}$C NMR spectra of complexes **1** and **2** in DMSO-$d_6$ were recorded with a Bruker Avance 400 MHz spectrometer; chemical shifts are reported relative to tetramethylsilane. Electrospray ionization (ESI) mass spectra were taken on a 7T-Fourier-transform ion cyclotron resonance (FT-ICR) mass spectrometer (APEX II, Bruker Daltonik) from solutions of complexes **1** and **2** prepared in DMSO. UV−vis spectra were recorded as Nujol mulls and in DMSO solution at concentrations in the range from 10$^{-5}$ to 5 × 10$^{-3}$ M on a Hitachi U-2001 dual-beam spectrophotometer. Molar conductivity measurements of 1 mM DMSO solutions of the complexes were carried out with a Crison Basic 30 conductometer. Fluorescence spectra were recorded in solution on a Hitachi F-7000 fluorescence spectrophotometer. Viscosity experiments were carried out using an ALPHA L Fungilab rotational viscometer equipped with an 18 mL LCP spindle.

**Table 1. Crystallographic Data for Complexes 1 and 2**

| parameter | 1 | 2 |
|---|---|---|
| formula | $C_9H_{10}PdN_3O_2Cl$ | $C_9H_{10}PtN_3O_2Cl$ |
| $M$/g mol$^{-1}$ | 334.05 | 422.74 |
| cryst syst | orthorhombic | orthorhombic |
| space group | $Pna2_1$ | $Pna2_1$ |
| $a$/Å | 6.8389(4) | 6.9452(2) |
| $b$/Å | 13.8406(7) | 10.9950(3) |
| $c$/Å | 10.9849(6) | 13.7541(3) |
| $\alpha = \beta = \gamma$/deg | 90 | 90 |
| $V$/Å$^3$ | 1039.77(10) | 1050.30(5) |
| $Z$ | 4 | 4 |
| $T$/K | 150(2) | 160(2) |
| $\lambda$/Å | 0.77490[a] | 1.54178[b] |
| $\rho_{calc}$/g cm$^{-3}$ | 2.134 | 2.673 |
| $\mu$/mm$^{-1}$ | 2.530 | 27.262 |
| measd/independent ($R_{int}$) reflns | 9175/3085 (0.0316) | 6417/1733 (0.0902) |
| obsd reflns [$I > 2\sigma(I)$] | 9286 | 1658 |
| $R_1$[c] | 0.0261 | 0.0376 |
| $wR_2$[d] | 0.0691 | 0.0856 |
| GOF on $F^2$ | 1.055 | 1.045 |
| $(\Delta\rho)_{max,min}$/e Å$^{-3}$ | 0.445, −0.570 | 1.589, −2.096 |

[a]Synchrotron, ALS beamline 11.3.1, silicon 111 monochromator. [b]Cu K$\alpha$ radiation, graphite monochromator. [c]$I > 2\sigma(I)$. $R_1 = \Sigma(||F_o| - |F_c||)/\Sigma|F_o|$. [d]$wR_2 = [\Sigma[w(F_o^2 - F_c^2)^2]/\Sigma[w(F_o^2)^2]]^{1/2}$, $w = 1/[\sigma^2(F_o^2) + [(ap)^2 + bp]$, where $p = [\max(F_o^2, 0) + 2F_c^2]/3$.

Cyclic voltammetry studies were performed on an Eco chemie Autolab Electrochemical analyzer. Cyclic voltammetric experiments were carried out in a 30 mL three-electrode cell. The working electrode was platinum disk, a separate Pt single-sheet electrode was used as the counter electrode, and a Ag/AgCl electrode saturated with KCl was used as the reference electrode. Cyclic voltammograms of the complexes were recorded in 0.4 mM DMSO solutions and 0.4 mM 1/2 DMSO/buffer solutions at $\nu$ = 100 mV s$^{-1}$, where TEAP (tetraethylammonium perchlorate) and the buffer solution were the supporting electrolytes, respectively. Oxygen was removed by purging the solutions with pure nitrogen which had been previously saturated with solvent vapors. All electrochemical measurements were performed at 25.0 ± 0.2 °C.

**Albumin Binding Studies.** The protein binding study was performed by tryptophan fluorescence quenching experiments using bovine (BSA, 3 $\mu$M) or human serum albumin (HSA, 3 $\mu$M) in buffer (containing 15 mM trisodium citrate and 150 mM NaCl at pH 7.0). Quenching of the emission intensity of tryptophan residues of BSA at 343 nm or HSA at 351 nm was monitored using the compounds as quenchers with increasing concentration (up to 2.2 × 10$^{-5}$ M). Fluorescence spectra were recorded from 300 to 500 nm at an excitation wavelength of 296 nm.[29] Fluorescence spectra of compounds were recorded under the same experimental conditions, and a low-intensity maximum emission appeared at 330 nm. Therefore, quantitative studies of the serum albumin fluorescence spectra were performed after their correction by subtracting the spectra of the compounds.

**DNA-Binding Studies.** Interaction of the ligand dapdoH$_2$ and complexes **1** and **2** with CT DNA has been studied with UV spectroscopy in order to investigate the possible binding modes to CT DNA and calculate the binding constants to CT DNA ($K_b$). Spectra of a CT DNA solution in the presence of each compound have been recorded for a constant CT DNA concentration in diverse [compound]/[CT DNA] mixing ratios ($r$) up to the value $r$ = 0.02. Binding constants, $K_b$, of the compounds with CT DNA have been determined using the UV spectra of the compound recorded for a constant concentration in the absence or presence of CT DNA for


dx.doi.org/10.1021/ic300739x | Inorg. Chem. 2012, 51, 7699−7710

diverse $r$ values in the range 0.03−1.0. Control experiments with DMSO did not show any changes in the spectra of CT DNA.

Viscosity experiments were carried out using an ALPHA L Fungilab rotational viscometer equipped with an 18 mL LCP spindle, and measurements were performed at 100 rpm. The viscosity of a DNA solution (0.1 mM) has been measured in the presence of increasing amounts of the compounds (0.1 mM). The relation between the relative solution viscosity $(\eta/\eta_0)$ and DNA length $(L/L_0)$ is given by the equation $L/L_0 = (\eta/\eta_0)^{1/3}$, where $L_0$ denotes the apparent molecular length in the absence of the compound.[30] The obtained data are presented as $(\eta/\eta_0)^{1/3}$ versus $r$, where $\eta$ is the viscosity of DNA in the presence of compound and $\eta_0$ is the viscosity of DNA alone in buffer solution.

Interaction of the complexes with CT DNA has been also investigated by monitoring the changes observed in the cyclic voltammogram of a 0.40 mM 1:2 DMSO:buffer solution of complex upon addition of CT DNA at diverse $r$ values. The buffer was also used as the supporting electrolyte, and cyclic voltammograms were recorded at $\nu = 100$ mV $s^{-1}$.

Competitive studies of each compound with ethidium bromide (EB) have been investigated with fluorescence spectroscopy in order to examine whether the compound can displace EB from its CT DNA−EB complex. The CT DNA−EB complex was prepared by adding 20 $\mu$M EB and 26 $\mu$M CT DNA in buffer (150 mM NaCl and 15 mM trisodium citrate at pH 7.0). The intercalating effect of the compound with the DNA−EB complex was studied by adding a certain amount of a solution of the compound step by step (up to $r$ = 0.65) into the solution of the DNA−EB complex. The influence of the addition of each compound to the DNA−EB complex solution has been obtained by recording the variation of fluorescence emission spectra.

## RESULTS AND DISCUSSION

**Syntheses, IR, and Mass Spectra.** Many synthetic procedures to oligo- and polynuclear transition metal complexes rely on reactions of simple metal sources, such as metal halides, carboxylates, or $\beta$-diketonates, with a potentially chelating/bridging ligand.[31] This route is also known from our previous work to yield structurally interesting 3d-metal complexes using several 2-pyridyl oxime[7b,c] and pyridyl dioxime[8] ligands. In the present study we investigated reactions between the relatively unexplored 2,6-diacetylpyridine dioxime ($dapdoH_2$) ligand and simple $Pd^{II}$ and $Pt^{II}$ halide sources.

Various reactions have been systematically explored with differing reagent ratios, reaction solvents, and other conditions. Reaction of $PdCl_2$ with $dapdoH_2$ in a 1:2 molar ratio in MeOH gave a yellow slurry, which was refluxed for a prolonged time to give a final orange solution. Slow evaporation of the resulting solution led to subsequent isolation of well-formed orange, needle-shaped crystals of the complex [PdCl(dapdoH)] (**1**) in very good yield (∼70%). When the same reaction and crystallization process were repeated using $PtCl_2$ in place of $PdCl_2$, the isostructural compound [PtCl(dapdoH)] (**2**) was isolated as dark red, plate-like crystals in excellent yield (∼80%). Formation of **1** and **2** is summarized in eq 1. It is noteworthy that for syntheses of both compounds **1** and **2** high-temperature conditions (i.e., reflux) were employed in order to enhance the solubility of the $PdCl_2$ and $PtCl_2$ starting materials and thus lead the reactions to the corresponding products formation.

$$MCl_2 + dapdoH_2 \xrightarrow[\text{reflux}]{\text{MeOH}} [MCl(dapdoH)] + HCl$$
$$M = Pd(\mathbf{1});\ Pt(\mathbf{2}) \qquad (1)$$

The "wrong" reaction ratio employed for preparation of both complexes, compared to the stoichiometric ratio (1:1) required by eq 1, obviously did not prove detrimental to formation of the products. The "correct" stoichiometric ratio, i.e., $M^{II}$:$dapdoH_2$ = 1:1, was also employed and led to the pure compounds albeit in much lower yields (∼30−35%). We also investigated the identity of the products as a function of the reaction solvent employed, but we obtained analogous products to **1** and **2** in every case from a variety of organic solvents, i.e., EtOH, MeCN, and $MeNO_2$.

The most noticeable feature of this reaction scheme is the single deprotonation of the dioximato group without the presence of a base in the reaction system. This is likely due to a metal-assisted polarization of the >N−OH bond upon coordination of the oxime N atoms with the metal center, which lowers the $pK_a$ of the first −OH group of the neutral $dapdoH_2$ ligand and thus favors its deprotonation.[22,32] We further targeted the double deprotonation of $dapdoH^-$ by reaction of **1** and **2** with 1−3 equiv of external base, such as $NEt_3$ or MOH (M = Li, Na); however, such reactions gave insoluble amorphous powders that perhaps were polymeric and not further characterized.

Magnetic susceptibility measurements were also performed and show that both complexes are diamagnetic, as expected (vide infra). Compounds **1** and **2** are stable, crystalline solids at room temperature and nonsensitive toward air and moisture. They are both soluble in DMF and DMSO and insoluble in almost all common organic solvents such as $CHCl_3$, benzene, and toluene.

The presence of a neutral oxime group in the single-deprotonated form of the ligand $dapdoH^-$ in both complexes is manifested by a broad IR band of medium intensity at 3442 (for **1**) and 3448 (for **2**) $cm^{-1}$, assigned to $\nu(OH)_{oxime}$.[33] Their broadness and relatively low frequency are both indicative of hydrogen bonding. The in-plane deformation mode of the 2-pyridyl ring of free $dapdoH_2$ at 686 $cm^{-1}$ [22] shifts upward in the spectra of **1** (708 $cm^{-1}$) and **2** (710 $cm^{-1}$), confirming involvement of the ring-N atom in coordination.[34] Several bands appear in the 1590−1390 $cm^{-1}$ region for the two complexes; contributions from $\nu(C{=}N)_{oximate}$, $\delta(CH_3)$, and $\delta(OH)$ (>1570 $cm^{-1}$) are expected in this region, but overlap with the stretching vibrations of the aromatic $dapdoH^-$ ring renders assignments and discussion of the coordination shifts difficult. The medium-intensity band at 1090 $cm^{-1}$ for free $dapdoH_2$ has been assigned to the $\nu(NO)_{oxime}$ mode.[22] The wavenumber of this vibration only slightly increases to ∼1094 and ∼1096 $cm^{-1}$ in **1** and **2**, respectively. This essentially negligible shift to higher frequencies has been discussed and is in accordance with the absence of oximate-*O* coordination with the metal center.[35] Finally, strong-intensity bands at 290−330 $cm^{-1}$ are present in the spectra of **1** and **2**; these bands are tentatively assigned to a vibration involving a $M^{II}$−$Cl^-$ (M = Pd, Pt) stretch.[36]

Formation of complexes **1** and **2** was further supported by detection of peaks in ESI mass spectra that correspond to the general formula [MCl(dapdoH)]. NMR results for both compounds in DMSO-$d_6$ are also consistent with the ESI-MS data, indicating retention of their structures in solution (vide infra).

**Description of Structures.** Both complexes crystallize in the orthorhombic space group $Pna2_1$, with the mononuclear [MCl(dapdoH)] (M = Pd (**1**); Pt (**2**)) molecules in a general position. The structures of **1** and **2** are shown in Figures 2 and


dx.doi.org/10.1021/ic300739x | Inorg. Chem. 2012, 51, 7699−7710

3, respectively. Selected interatomic distances and angles for **1** and **2** are listed in Tables 2 and 3, respectively.

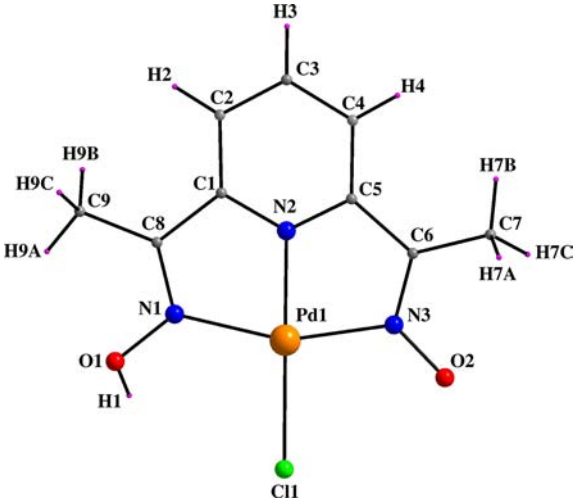


**Figure 2.** Labeled PovRay representation of complex **1**.

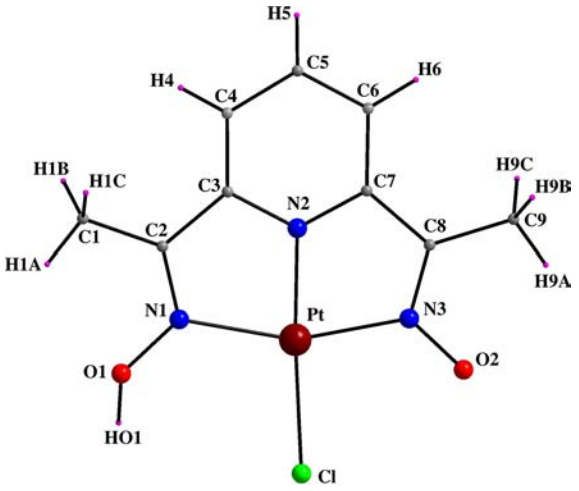


**Figure 3.** Labeled PovRay representation of complex **2**.

**Table 2. Selected Bond Lengths (Angstroms) and Angles (degrees) for Complex 1**

| | | | |
|---|---|---|---|
| Pd(1)–N(1) | 2.069(2) | Pd(1)–Cl(1) | 2.2906(7) |
| Pd(1)–N(2) | 1.936(2) | N(1)–O(1) | 1.370(3) |
| Pd(1)–N(3) | 2.007(3) | N(3)–O(2) | 1.305(3) |
| N(1)–Pd(1)–N(2) | 78.79(10) | N(2)–Pd(1)–N(3) | 80.62(10) |
| N(1)–Pd(1)–N(3) | 159.39(8) | N(2)–Pd(1)–Cl(1) | 173.19(5) |
| N(1)–Pd(1)–Cl(1) | 103.08(6) | N(3)–Pd(1)–Cl(1) | 97.49(6) |

**Table 3. Selected Bond Lengths (Angstroms) and Angles (degrees) for Complex 2**

| | | | |
|---|---|---|---|
| Pt–N(1) | 2.058(7) | Pt–Cl | 2.290(3) |
| Pt–N(2) | 1.902(9) | N(1)–O(1) | 1.360(9) |
| Pt–N(3) | 2.009(9) | N(3)–O(2) | 1.315(9) |
| N(1)–Pt–N(2) | 80.0(4) | N(2)–Pt–N(3) | 79.9(3) |
| N(1)–Pt–N(3) | 159.8(3) | N(2)–Pt–Cl | 173.8(2) |
| N(1)–Pt–Cl | 102.7(2) | N(3)–Pt–Cl | 97.4(2) |

The $Pd^{II}$ center in **1** is coordinated by a terminal chloro group and a *N*,*N*′,*N*″-tridentate chelating ($\eta^3$) dapdoH$^-$ ligand. The dapdoH$^-$ donor atoms are the two nitrogen atoms of the oxime/oximate moiety (N1, N3) and the nitrogen atom of the pyridyl group (N2). Thus, the $Pd^{II}$ atom is four coordinate, and the tetrahedrality calculated for complex **1** gives a dihedral angle of 6.5° (the tetrahedrality for a four-coordinate complex can be determined from the angle subtended by two planes, each encompassing the metal and two adjacent atoms; for strictly square planar complexes with $D_{4h}$ symmetry, the tetrahedrality is 0°; for tetrahedral complexes with $D_{2d}$ symmetry, the tetrahedrality equals 90°), supporting a distorted square planar geometry for the basal plane $PdN_3Cl$.[30] Additionally, the *cis* and *trans* angles lie in the 78.8–103.1° and 159.4–173.2° ranges, deviating only slightly from the 90° and 180° values, respectively, of an ideal square plane. This deviation is likely due to formation of two, five-membered chelating rings around the $Pd^{II}$ ion, giving rise to an overall, nonsymmetric $PdN_3Cl$ chromophore. The two five-membered chelating rings, Pd1–N1–C8–C1–N2 and Pd1–N2–C5–C6–N3, share the common Pd1–N2 edge. The dihedral angle formed between the mean planes Pd1–N1–C8–C1–N2 and Pd1–N2–C5–C6–N3 is 1.2°. The N1···N2 and N2···N3 bite distances (2.544(3) and 2.552(3) Å, respectively) lead to N1–Pd1–N2 and N2–Pd1–N3 angles (78.8(1)° and 80.6(1)°, respectively), appreciably less than the ideal 90°. Such small bite angles are typical for metal complexes with N-donor chelating ligands.[37]

The pyridyl nitrogen atom can be viewed as strongly coordinating to the metal [Pd1–N2 = 1.936(2) Å)], while the chloride ion forms a weaker bond to $Pd^{II}$ [Pd1–Cl1 = 2.2906(7) Å], in accordance with Pd–Cl distances reported in the literature.[36,38] The four donor atoms are not coplanar; N1 and N3 lie 0.054 and 0.057 Å, respectively, above the best least-squares plane through the four atoms, while N2 and Cl1 lie 0.070 and 0.042 Å, respectively, below it; the $Pd^{II}$ atom is 0.063 Å above the plane. There are four symmetry-equivalent, interionic OH···O and OH···Cl hydrogen bonds involving the protonated dapdoH$^-$ O atom as donor and deprotonated dapdoH$^-$ O atom and Cl$^-$ group of adjacent molecules as acceptors. Their dimensions are as follows: O(1)···O(2′) 2.571(3) Å, H(1)···O(2′) 1.736(3) Å, O(1)–H(1)···O(2′) 172.5(1)° and O(1)···Cl(1′) 3.253(1) Å, H(1)···Cl(1′) 3.073(1) Å, O(1)–H(1)···Cl(1′) 94.8(1)°. These H bonds serve to link neighboring $Pd^{II}$ monomers into one-dimensional, zigzag chains along the *c* axis (Figure S1, Supporting Information, top) and their existence rationalizes the high thermodynamic stability of **1**.

The structure of complex **2** (Figure 3) is very similar to that of **1**, with the only main difference being the nature of the metal ion, i.e., $Pt^{II}$ instead of $Pd^{II}$. Thus, the $Pt^{II}$ atom is again four coordinate with a distorted square planar geometry (the tetrahedrality of the basal plane is equal to 5.6°) and nonsymmetric $PtN_3Cl$ chromophore: the cis and trans angles lie in the 79.9–102.7° and 159.8–173.8° ranges. The pyridyl nitrogen atom can be viewed as strongly coordinating to the metal [Pt–N2 = 1.902(9) Å)], while the chloride ion forms a weaker bond to $Pt^{II}$ [Pt–Cl = 2.290(3) Å] similar to that found in **1**. The four donor atoms are again not coplanar; N1 and N3 lie 0.039 and 0.042 Å, respectively, above the best least-squares plane through the four atoms, while N2 and Cl lie 0.051 and 0.030 Å, respectively, below it; the $Pt^{II}$ atom is 0.059 Å above the plane. Finally, there are also four symmetry-equivalent, interionic OH···O and OH···Cl hydrogen bonds, similar in nature with those seen in **1**, serving to link neighboring $Pd^{II}$


dx.doi.org/10.1021/ic300739x | *Inorg. Chem.* 2012, 51, 7699–7710

monomers into one-dimensional, zigzag chains along the *c* axis (Figure S1, Supporting Information, bottom). Their dimensions are as follows: O(1)···O(2′) 2.543(5) Å, HO(1)···O(2′) 1.484(5) Å, O(1)−HO(1)···O(2′) 157.5(1)° and O(1)···Cl′ 3.260(1) Å, HO(1)···Cl′ 3.017(1) Å, O(1)−OH(1)···Cl′ 92.6(1)°.

In general lines, there are no structurally characterized palladium(II) and platinum(II) complexes bearing any kind of pyridyl dioxime ligands. Complexes **1** and **2** are the first structurally characterized $Pd^{II}$ and $Pt^{II}$ compounds that contain any form (neutral, mono- or dianionic) of the 2,6-diacetylpyridine dioxime ligand. They are also rare examples of mononuclear, neutral molecular species containing the $MN_3Cl$ chromophore (M = Pd,[39] Pt[40]) with the three N atoms arising from a tridentate chelating ligand. Among these, only two $Pt^{II}$ complexes have been biologically studied,[40a,b] albeit none of them include an oximate ligand.

**NMR Spectroscopy Studies.** The $^1H$ and $^{13}C$ NMR chemical shifts of $dapdoH_2$ in DMSO-$d_6$ have been previously reported and discussed in detail.[22] The solubilities of **1** and **2** in common organic solvents were too low to allow other than DMSO-$d_6$ solutions to be prepared and studied. The representative $^1H$ NMR chemical shifts of both complexes in DMSO-$d_6$ are given in Table 4. In general, the chemical shifts of ligand protons bound to diamagnetic metal ions are influenced by three factors:[41] (i) the electron density on the ligand diminishes upon coordination, inducing a downfield shift; (ii) steric effects lead to a downfield shift; (iii) alignment of a proton above an adjacent aromatic ring leads to a dramatic upfield shift. $^1H$ NMR spectra of **1** and **2** were assigned with the aid of recent studies of coordinated $dapdoH_2$ and a number of diamagnetic metal complexes with related ligands.[22]

**Table 4. $^1H$ NMR Data[a] for the Free Ligand $dapdoH_2$ and Complexes 1 and 2**

| compound | NO-H | py-3(5)H | py-4H | $-CH_3$ |
|---|---|---|---|---|
| $dapdoH_2$ | 11.52 | 7.78 | 7.64 | 2.23 |
| **1** | 12.53 | 7.97 | 8.14 | 2.40 |
| **2** | 12.58 | 7.94 | 8.11 | 2.37 |

[a]In DMSO-$d_6$ at 400 MHz. Chemical shifts ($\delta$ values) are given in ppm relative to $Me_4Si$. Spectra recorded at ambient temperature.

As expected, the electron density on the pyridine ring of $dapdoH_2$ diminishes upon coordination to the metal centers. Thus, a downfield shift of the pyridine proton resonances is observed for both complexes compared to the free ligand. The effect is greater for the proton in the 4 position than for the protons in 3(5) positions, resulting in a reversal of their relative positions compared to the free ligand.[22,32] A relatively large downfield shift is also observed for the oxime proton upon coordination of the metal ion, in agreement with the greater acidity observed for the oxime protons for the metal compounds of $dapdoH_2$. Another reason for the appearance of the oxime proton at a low field in the spectra of both **1** and **2** might be the steric hindrance from the chloro ligand (observed in the solid state structure).[36a]

**UV−Vis Spectroscopy.** The UV−vis spectra as Nujol mulls and in DMSO solutions show a similar pattern, supporting the integrity of complexes in solution. In the visible region, two low-intensity bands are observed at 563 ($\varepsilon$ = 150 $M^{-1}$ $cm^{-1}$) and 520 nm ($\varepsilon$ = 120 $M^{-1}$ $cm^{-1}$) for **1** and 575 ($\varepsilon$ = 40 $M^{-1}$ $cm^{-1}$) and 539 nm ($\varepsilon$ = 400 $M^{-1}$ $cm^{-1}$) for **2**. These two bands may be attributed to d−d transitions and are within the range observed for square planar Pt(II) and Pd(II) complexes with $d^8$ configuration.[42] Additionally, the band observed in the range 391−395 nm ($\varepsilon$ = 850−1750 $M^{-1}$ $cm^{-1}$) may be assigned to charge-transfer transition.

In order to explore the stability of complexes in buffer solution, UV−vis spectra in the series of pH (pH range 6−8, since the biological experiments are performed at pH = 7) with the use of diverse buffer solutions (150 mM NaCl and 15 mM trisodium citrate at pH values regulated by HCl solution) have also been recorded. No significant changes (shift of the $\lambda_{max}$ or new peaks) have been observed (Figure S2, Supporting Information), indicating that the complexes keep their integrity in the pH range 6−8. The fact that the complexes are nonelectrolytes in DMSO solution ($\Lambda_M$ = 7−12 mho $cm^2$ $mol^{-1}$, in 1 mM DMSO solution) and have the same UV−vis spectral pattern in Nujol and DMSO solution as well as in the presence of the buffer solution suggests that the compounds are stable and keep their integrity in solution. It should be also noted that a similar conclusion arose from the above NMR studies.

**Biological Studies.** The general procedures related to the study of the interaction of complexes **1** and **2**, as well as that of the free ligand $dapdoH_2$, with the serum albumins binding by tryptophan fluorescence quenching experiments[30,43−45] and with CT DNA[46,47] by UV spectroscopy,[48,49] viscosity experiments[50] and cyclic voltammetry as well as their competitive

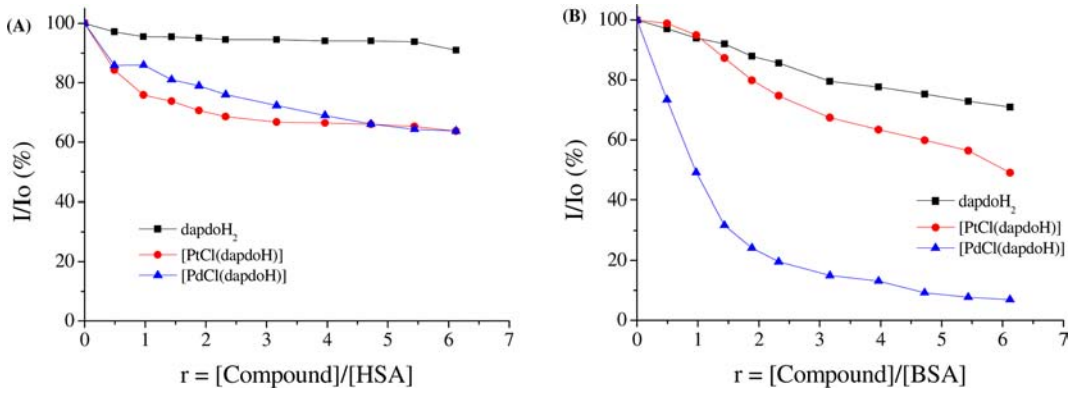


**Figure 4.** Plot of % relative fluorescence intensity at (A) $\lambda_{em}$ = 351 nm (%) vs *r* (*r* = [compound]/[HSA]) and (B) $\lambda_{em}$ = 343 nm (%) vs *r* (*r* = [compound]/[BSA]) for the compounds in buffer solution (150 mM NaCl and 15 mM trisodium citrate at pH 7.0).


dx.doi.org/10.1021/ic300739x | *Inorg. Chem.* 2012, 51, 7699−7710

**Table 5. HSA and BSA Binding Constants and Parameters ($K_{SV}$, $k_q$, $K$, $n$) Derived for the Free Ligand and the Reported Compounds 1 and 2**

| compound | $K_{SV}$ ($M^{-1}$) | $k_q$ ($M^{-1}$ $s^{-1}$) | $K$ ($M^{-1}$) | $n$ |
|---|---|---|---|---|
| HSA | | | | |
| $dapdoH_2$ | $4.52(\pm0.70)\times10^3$ | $4.52(\pm0.07)\times10^{11}$ | $4.57(\pm0.25)\times10^5$ | 0.07 |
| [PdCl(dapdoH)] | $2.89(\pm0.20)\times10^4$ | $2.89(\pm0.20)\times10^{12}$ | $1.23(\pm0.09)\times10^5$ | 0.53 |
| [PtCl(dapdoH)] | $4.94(\pm0.25)\times10^4$ | $4.94(\pm0.25)\times10^{12}$ | $4.54(\pm0.27)\times10^5$ | 0.40 |
| BSA | | | | |
| $dapdoH_2$ | $2.31(\pm0.08)\times10^4$ | $2.31(\pm0.08)\times10^{12}$ | $3.13(\pm0.22)\times10^4$ | 0.81 |
| [PdCl(dapdoH)] | $7.70(\pm0.25)\times10^5$ | $7.70(\pm0.25)\times10^{13}$ | $4.48(\pm0.21)\times10^5$ | 1.05 |
| [PtCl(dapdoH)] | $5.49(\pm0.25)\times10^4$ | $5.49(\pm0.25)\times10^{12}$ | $5.50(\pm0.65)\times10^4$ | 0.92 |

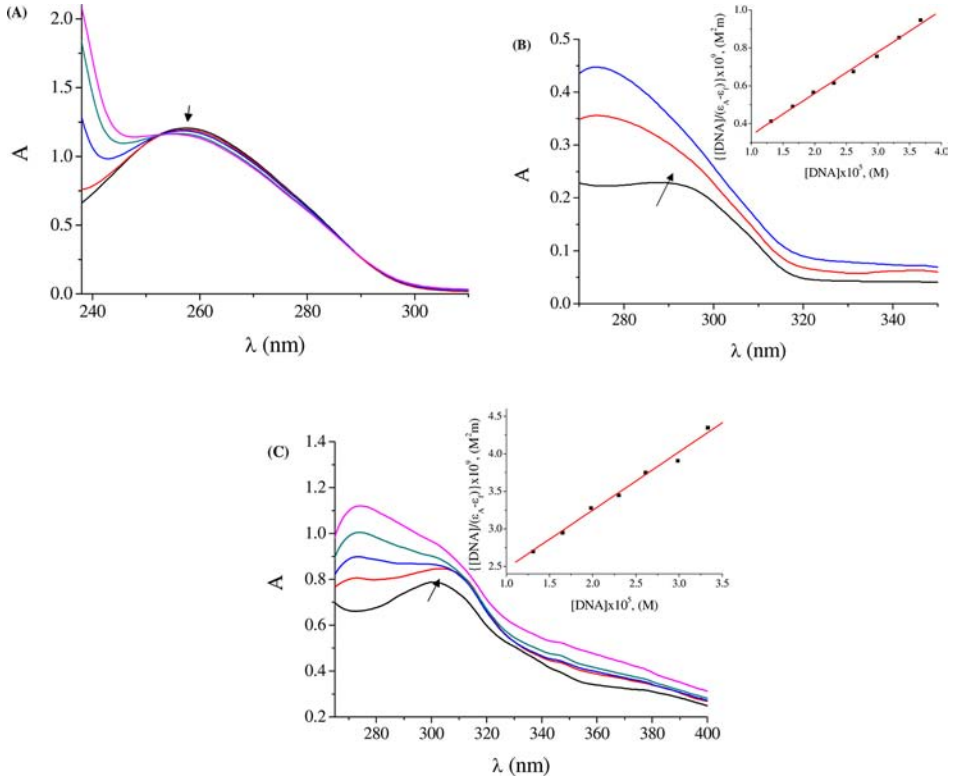


**Figure 5.** (A) UV spectra of CT DNA ($1.8\times10^{-4}$ M) in buffer solution (150 mM NaCl and 15 mM trisodium citrate at pH 7.0) in the absence or presence of [PtCl(dapdoH)] (**2**). Arrows show the changes upon increasing amounts of compound. (B) UV spectra of $dapdoH_2$ in DMSO solution ($1\times10^{-5}$ M) in the presence of CT DNA at increasing amounts. (C) UV spectra of [PdCl(dapdoH)] (**1**) in DMSO solution ($1\times10^{-5}$ M) in the presence of CT DNA at increasing amounts. Arrows in B and C show the changes upon increasing amounts of CT DNA. Insets in B and C: plot of $([DNA])/(\varepsilon_A - \varepsilon_f)$ vs [DNA].

studies with ethidium bromide by fluorescence spectroscopy[51−53] have been thoroughly described in the corresponding references.

**Binding to Serum Albumins.** Serum albumin (SA) is the most abundant protein in plasma and is involved in the transport of drugs, metal ions, and compounds through the bloodstream. Bovine serum albumin (BSA) is the most extensively studied serum albumin, due to its structural homology with human serum albumin (HSA). Addition of the compounds to HSA results in a low to relatively moderate fluorescence quenching at $\lambda_{em}$ = 351 nm, reaching up to 9% for $dapdoH_2$ and 36% for **1** and **2**, as calculated after correction of the initial fluorescence spectra (Figure 4A). The observed quenching may be attributed to possible changes in protein secondary structure leading to changes in the tryptophan environment of HSA, thus indicating binding of each compound to HSA.[44]

The Stern−Volmer and Scatchard equations and graphs may be often used in order to study the interaction of a quencher with SAs. According to Stern−Volmer quenching equation, eq 2[30,54]

$$\frac{I_o}{I} = 1 + k_q\tau_0[Q] = 1 + K_{SV}[Q] \quad (2)$$

the dynamic quenching constant ($K_{SV}$, $M^{-1}$) may be obtained by the slope of the diagram $I_o/I$ vs [Q], where $I_o$ is the initial tryptophan fluorescence intensity of SA, $I$ is the tryptophan fluorescence intensity of SA after addition of the quencher (ligand or complexes), $k_q$ is the quenching rate constants of SA, $K_{SV}$ is the dynamic quenching constant, $\tau_o$ is the average lifetime of SA without the quencher ($\tau_o$ of tryptophan in SA at $\sim10^{-8}$ s), and [Q] is the concentration of the quencher. The approximate quenching constant $k_q$ ($M^{-1}$ $s^{-1}$) may be calculated from eq 3


dx.doi.org/10.1021/ic300739x | Inorg. Chem. 2012, 51, 7699−7710

$$K_{SV} = k_q \tau_o \quad (3)$$

The calculated $K_{SV}$ and $k_q$ values (Table 5) for interaction of the free ligand and complexes **1** and **2** with HSA (Figure S3, Supporting Information) indicate good HSA propensity of the compounds, with [PtCl(dapdoH)] (**2**) exhibiting the strongest quenching ability ($k_q = 4.94(\pm 0.25) \times 10^{12}$ $M^{-1}$ $s^{-1}$). $k_q$ values are higher than diverse kinds of quenchers for biopolymers fluorescence ($2.0 \times 10^{10}$ $M^{-1}$ $s^{-1}$), indicating the existence of a static quenching mechanism.[45]

From the Scatchard equation, eq 4[30]

$$\frac{\Delta I/I_o}{[Q]} = nK - K\frac{\Delta I}{I_o} \quad (4)$$

the association binding constant $K$ ($M^{-1}$) may be calculated from the slope in plots $(\Delta I/I_o)/([Q])$ versus $\Delta I/I_o$ (Figure S4, Supporting Information), while the number of binding sites per albumin, $n$, is given by the ratio of the $y$ intercept to the slope.[30] The association binding constants ($K$) of the compounds (Table 5) are moderate to high, and dapdoH$_2$ and **2** have the highest $K$ values among the compounds. Comparison of the $n$ values reveals that both complexes **1** and 2 exhibit significantly higher $n$ values than the free ligand.

The quenching provoked by the compounds to the BSA fluorescence at $\lambda = 343$ nm (Figure 4B) is more significant than HSA and reaches up to 71% of the initial fluorescence intensity for dapdoH$_2$, 7% for **1**, and 49% for **2**, indicating that the binding of each compound to BSA quenches the intrinsic fluorescence of the tryptophans in BSA.[55] The calculated values of $K_{SV}$ and $k_q$ for the compounds, as obtained by the slope of the Stern−Volmer plot (Figure S5, Supporting Information), indicate their good BSA binding propensity, with complex **1** exhibiting significantly higher quenching ability (Table 5). From the Scatchard plots (Figure S6, Supporting Information), the $K$ and $n$ values of each compound for BSA have been calculated (Table 5), with **1** exhibiting the highest association binding constant and $n$ value to BSA among the compounds.

Comparing the affinity of the complexes for BSA and HSA ($K$ values), it is obvious that the free ligand dapdoH$_2$ and complex [PtCl(dapdoH)] (**2**) show higher affinity for HSA than BSA while [PdCl(dapdoH)] (**1**) shows higher affinity for BSA than HSA. The binding constant ($K$) between a compound and serum albumins should be less than one of the highest protein−ligands binding affinity ($K_{avidin\text{-}ligands} \approx 10^{15}$ $M^{-1}$) observed in order to get released from the albumins to the target cells.[56a] In the case of a $K$ with a higher value than $K_{avidin\text{-}ligands} \approx 10^{15}$ $M^{-1}$, the compound cannot be released upon arrival to the target cells. It is obvious that $K$ values for dapdoH$_2$ and complexes **1** and **2**, lying in the range from $3.13 \times 10^4$ to $4.57 \times 10^5$ $M^{-1}$ (Table 5), are quite below this value, suggesting potential release from the albumins at the target cells. Therefore, interaction of compounds with albumins may provide useful information concerning any potential application.[56b]

**Study of the DNA Interaction with UV Spectroscopy.** UV spectra have been recorded for a constant CT DNA concentration in different [compound]/[DNA] mixing ratios ($r$). UV spectra of a solution of CT DNA in the presence of **2** derived for diverse $r$ values are shown representatively in Figure 5A, since the behavior of CT DNA in the presence of dapdoH$_2$ and **1** is similar. Their addition to a DNA solution results in a decrease of the intensity at $\lambda_{max} = 258$ nm, indicating that the interaction with CT DNA results in direct formation of a new complex with double-helical CT DNA.[46a]

In the UV spectra of the compounds, the intense absorption bands observed are attributed to the intraligand transition of the characteristic groups of the coordinated ligand. Any interaction between each compound and CT DNA could perturb the intraligand-centered spectral transitions as observed in the UV spectra of a $1 \times 10^{-5}$ M solution of the compounds upon addition of CT DNA in diverse $r$ values.[57] In the UV spectra of dapdoH$_2$, the band centered at 293 nm exhibits, in the presence of increasing amounts of CT DNA, a significant hyperchromism (Figure 5B) which may suggest tight binding to CT DNA probably by external interaction.[58] Similarly, in the UV spectra of **2**, the bands centered at 297 and 335 nm, in the presence of increasing amounts of CT DNA, do not shift, exhibiting a lower hyperchromism. For **1**, the band centered at 300 nm exhibits, in the presence of increasing amounts of CT DNA, a hyperchromism accompanied by a red shift of 7 nm (up to 307 nm) while the band at 338 nm presents a hyperchromism without any change of the position (Figure 5C).

The results derived from the UV titration experiments suggest that the compounds can bind to CT DNA.[59] The hyperchromism observed may be a first evidence of possible external binding to CT DNA, while the existence of a red shift for **1** may suggest stabilization upon binding to DNA; in such case, intercalation due to $\pi \rightarrow \pi^*$ stacking interactions between the base pairs of CT DNA may not be ruled out.[60] Nevertheless, the exact mode of binding cannot be merely proposed by UV spectroscopic titration studies. The binding constant of the compounds to CT DNA ($K_b$) is obtained by the ratio of the slope to the $y$ intercept in plots $([DNA])/(\varepsilon_A - \varepsilon_f)$ versus [DNA][48] according to eq 5

$$\frac{[DNA]}{(\varepsilon_A - \varepsilon_f)} = \frac{[DNA]}{(\varepsilon_b - \varepsilon_f)} + \frac{1}{K_b(\varepsilon_b - \varepsilon_f)} \quad (5)$$

where [DNA] is the concentration of DNA in base pairs, $\varepsilon_A = A_{obsd}/[compound]$, $\varepsilon_f$ is the extinction coefficient for the free compound, and $\varepsilon_b$ is the extinction coefficient for the compound in the fully bound form. The calculated $K_b$ values for the compounds (Table 6) suggest a strong binding to CT DNA.[23,30,60c] It is obvious from Table 6 that coordination of the dapdoH$_2$ to Pd(II) and Pt(II) in complex **1** or **2**, respectively, results in a slight or a more pronounced decrease of the $K_b$ value, respectively, since free dapdoH$_2$ exhibits the highest $K_b$ value ($=1.83(\pm 0.23) \times 10^5$ $M^{-1}$) among the compounds, which is (as well as the $K_b$ value of complex **2**) of the same magnitude to that of the classical intercalator EB ($K_b = 1.23(\pm 0.07) \times 10^5$ $M^{-1}$).[60,61]

**Table 6. DNA Binding Constants ($K_b$) of the Compounds and Stern−Volmer Constants ($K_{SV}$) for EB Displacement**

| compound | $K_b$ ($M^{-1}$) | $K_{SV}$ ($M^{-1}$) |
|---|---|---|
| dapdoH$_2$ | $1.83(\pm 0.23) \times 10^5$ | $1.20(\pm 0.05) \times 10^6$ |
| [PdCl(dapdoH)], **1** | $4.58(\pm 0.06) \times 10^4$ | $4.95(\pm 0.23) \times 10^5$ |
| [PtCl(dapdoH)], **2** | $1.13(\pm 0.08) \times 10^5$ | $3.64(\pm 0.13) \times 10^6$ |

**Cyclic Voltammetry and DNA-Binding Study.** Cyclic voltammograms of the complexes in DMSO solution show that they are redox active. Their electrochemical behavior and the corresponding potentials of each process are in accordance with similar Pt(II) and Pd(II) complexes previously reported. More


dx.doi.org/10.1021/ic300739x | Inorg. Chem. 2012, 51, 7699−7710

specifically, for [PtCl(dapdoH)] (**2**), all observed waves can be characterized as irreversible (Figure S7, Supporting Information). Two one-electron cathodic waves appear at −975 ($E_{pc1}$) and −1140 mV ($E_{pc2}$), which can be assigned to the process [Pt(II)] → [Pt(I)] and formation of [Pt(0)], respectively. On the reverse scan, two anodic waves at −440 (of low current, $E_{pa1}$) and +1400 mV ($E_{pa2}$) can be attributed to oxidation to [Pt(II)] and [Pt(IV)], respectively, followed by the presence of an intense cathodic wave at −590 mV ($E_{pc3}$, reduction of [Pt(IV)] to [Pt(II)]) upon second scan.[62]

In the case of [PdCl(dapdoH)] (**1**), the observed waves may be characterized as quasireversible or irreversible. Cyclic voltammograms of **1** exhibit two cathodic waves at −700 ($E_{pc1}$) and −1200 mV ($E_{pc2}$) which can be assigned to the process [Pd(II)] → [Pd(I)] and formation of [Pd(0)], respectively. On the reverse scan, the anodic waves at −490 (of low current, $E_{pa1}$), +750 ($E_{pa2}$), and +1335 mV ($E_{pa3}$) may be attributed to metal-based oxidation to Pd(II), Pd(III), and Pd(IV), respectively, and are followed in the second scan by reduction to Pd(II) species at −590 mV (Figure S8, Supporting Information).[42b,c,63]

Electrochemical investigations of metal−DNA interactions can provide a supplement to spectroscopic methods and yield useful information about interactions with both the reduced and the oxidized form of the metal. In general, the electrochemical potential of a small molecule will shift positively when it intercalates into DNA double helix, and it will shift to a negative direction in the case of electrostatic interaction with DNA. Upon addition of a CT DNA to a complex solution, new redox peaks did not appear and the current intensity decreased, suggesting the existence of an interaction between each complex and CT DNA. The decrease in current intensity can be explained in terms of an equilibrium mixture of free and DNA-bound complex to the electrode surface.[64]

For increasing amounts of CT DNA (Figures S9 and S10, Supporting Information), both the cathodic ($E_{pc}$) and the anodic ($E_{pa}$) potentials of **1** exhibit a positive shift ($\Delta E_p$) (Table 7), suggesting an intercalative mode of binding between

**Table 7. Cathodic and Anodic Potentials (in mV) for the Redox Couple M(II)/M(I) in 1/2 DMSO/Buffer Solution of the Complexes in the Absence and Presence of CT DNA**

| complex | $E_{pc(f)}$ [a] | $E_{pc(b)}$ [b] | $\Delta E_{pc}$ [c] | $E_{pa(f)}$ [a] | $E_{pa(b)}$ [b] | $\Delta E_{pa}$ [c] |
|---|---|---|---|---|---|---|
| [PdCl(dapdoH)], **1** | −691 | −686 | +5 | −556 | −548 | +8 |
| [PtCl(dapdoH)], **2** | −730 | −820 | −90 | −572 | −435 | +137 |

[a] $E_{pc/a}$ in DMSO/buffer solution in the absence of CT DNA ($E_{pc/a(f)}$). [b] $E_{pc/a}$ in DMSO/buffer solution in the presence of CT DNA ($E_{pc/a(b)}$). [c] $\Delta E_{pc/a} = E_{pc/a(b)} - E_{pc/a(f)}$.

the complexes and CT DNA bases.[30,65] In the case of **2**, the positive shift of $\Delta E_{pa}$ may suggest intercalation as a binding mode to CT DNA, while the negative shift of $\Delta E_{pc}$ may reveal the coexistence of a binding of the complex to the surface of CT DNA.

**DNA-Binding Study with Viscosity Measurements.** The viscosity of DNA is sensitive to its length changes; therefore, its measurement upon addition of a compound is often concerned to clarify the interaction mode of a compound with DNA. Viscosity measurements were carried out on CT DNA solutions upon addition of increasing amounts of the compounds. The DNA relative viscosity is increased upon addition of free dapdoH$_2$ or its complexes **1** and **2** (Figure 6), which can be explained by insertion of the compounds in

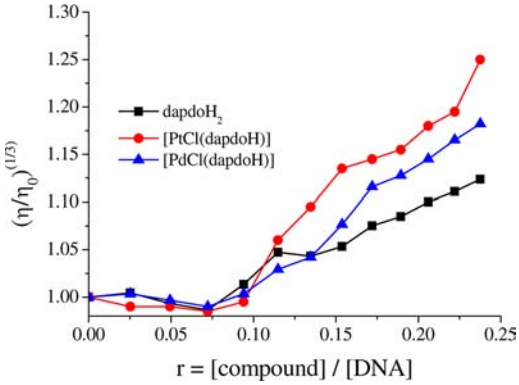


**Figure 6.** Relative viscosity of CT DNA $(\eta/\eta_o)^{1/3}$ in buffer solution (150 mM NaCl and 15 mM trisodium citrate at pH 7.0) in the presence of the compounds at increasing amounts ($r$).

between the DNA base pairs, leading to an increase in the separation of base pairs at intercalation sites and, thus, an increase in overall DNA length. Therefore, the existence of intercalation of the complexes into the DNA bases may be concluded as the most possible interaction mode to CT DNA.[30,43,50b,c]

**Competitive Studies with Ethidium Bromide.** The compounds show no fluorescence at room temperature in solution or in the presence of CT DNA, and their binding to DNA cannot be directly predicted through the emission spectra. On the other hand, free EB does not exhibit significant emission in buffer solution due to fluorescence quenching by the solvent molecules, while the fluorescence intensity is highly enhanced upon addition of CT DNA, due to its strong intercalation with DNA base pairs. Therefore, competitive EB binding studies may be carried out in order to examine the binding of each compound with DNA. Emission spectra of EB bound to CT DNA in the absence and presence of each complex have been recorded for [EB] = 20 $\mu$M, [DNA] = 26 $\mu$M for increasing amounts of each compound. Addition of each compound at diverse $r$ values results in significant quenching (~79% for dapdoH$_2$, 83.5% for [PtCl(dapdoH)] (**2**), and 86% for [PdCl(dapdoH)] (**1**)) of the emission band (Figure 7) of the DNA−EB system at 592 nm, indicating the

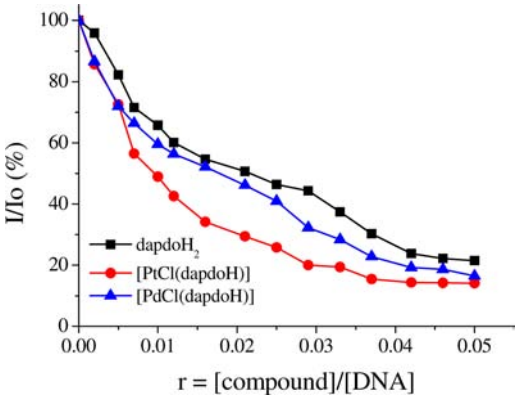


**Figure 7.** Plot of EB relative fluorescence intensity at $\lambda_{em}$ = 592 nm (%) vs $r$ ($r$ = [Compound]/[DNA]) for the compounds in buffer solution (150 mM NaCl and 15 mM trisodium citrate at pH 7.0).


dx.doi.org/10.1021/ic300739x | Inorg. Chem. 2012, 51, 7699−7710

strong ability of the compounds to displace EB from the DNA−EB complex. Thus, interaction of the complexes to CT DNA by the intercalative mode may be suggested.

In order to evaluate the quenching efficiency for each compound, the Stern−Volmer constant $K_{SV}$ is calculated by the slope of the diagram $I_o/I$ vs [Q] according to eq 6

$$\frac{I_o}{I} = 1 + K_{SV}[Q] \quad (6)$$

where $I_o$ and I are the emission intensities in the absence and presence of the quencher, respectively, and [Q] is the concentration of the quencher. The Stern−Volmer plots of DNA−EB (Figure S11, Supporting Information) illustrate that the quenching of EB bound to DNA by the compounds is in good agreement ($R$ = 0.99) with the linear Stern−Volmer equation, proving that replacement of EB bound to DNA by each compound results in a decrease in the fluorescence intensity.[66] The high $K_{SV}$ (Table 6) values of the compounds show that they can bind tightly to the DNA probably by intercalation.[60,65]

## CONCLUSIONS AND PERSPECTIVES

The present work extends the body of results that emphasize the ability of the pyridyl dioximate-based ligands to form interesting metal complexes, not only with 3d-metal ions exhibiting high nuclearities and impressive magnetic properties but also with 4d- and 5d-metal ions, providing access to a new biological perspective. The reported mononuclear compounds [PdCl(dapdoH)] (**1**) and [PtCl(dapdoH)] (**2**) are the first structurally characterized palladium(II) and platinum(II) complexes bearing any kind of pyridyl dioxime ligands. Detailed spectroscopic and physicochemical characterization of both compounds with a plethora of techniques revealed their integrity in DMSO solutions. UV study of the interaction of the free ligand $dapdoH_2$ and its complexes **1** and **2** with CT DNA has shown that the compounds can bind to CT DNA. Cyclic voltammograms of the complexes in the presence of CT DNA solution as well as viscosity measurements have shown that the interaction of the complexes with CT DNA is mainly through intercalation. Competitive studies with EB indicate that the complexes have the ability to displace the DNA-bound EB, suggesting competition with EB. Finally, both $dapdoH_2$ and its metal complexes **1** and **2** exhibit good binding affinity to human or bovine serum albumin proteins, having relatively high binding constant values.

As far as future perspectives are concerned, we are currently targeting selective replacement of the terminal $Cl^-$ ion in both **1** and **2**, through abstraction with a $Ag^+$ salt, with a neutral, monodentate N-donor ligand, such as pyridine, in order to isolate cationic mononuclear species with probably better solubilities and different biological properties, i.e., a different kind of binding to DNA. The cytotoxic and antibacterial activities, such as those against LMS and MCF-7 cells, flow cytometry analysis, as well as photophysical properties of both complexes **1** and **2** are also in progress, and the results will be reported in an upcoming full paper.

## ASSOCIATED CONTENT

### Supporting Information

X-ray crystallographic files in CIF format and various structural, spectroscopic, and physicochemical figures for complexes **1** and **2**. This material is available free of charge via the Internet at http://pubs.acs.org.

## AUTHOR INFORMATION

### Corresponding Author

*E-mail: thstama@chemistry.upatras.gr (T.C.S.); gepsomas@chem.auth.gr (G.P.).

### Notes

The authors declare no competing financial interest.

## ACKNOWLEDGMENTS

The Advanced Light Source is supported by The Director, Office of Basic Energy Sciences, of the U.S. Department of Energy under Contract No. DE-AC02-05CH11231. Th.C.S. thanks the Royal Society of Chemistry Research Fund for chemical supply. The authors wish to thank Dr. Konstantis F. Konidaris for recording the ESI mass spectra of both compounds.

## REFERENCES

(1) Pombeiro, A. J. L.; Kukushkin, V. Yu. in: McCleverty, J. A.; Meyer, T. J. (Eds.), *Comprehensive Coordination Chemistry II*, Vol. *1*, Elsevier, Amsterdam, 2004, p 631.

(2) Eyer, P. *Toxicol. Rev.* **2003**, *22*, 165.

(3) Black, R. M.; Harrison, J. M. "*The Chemistry of Organophosphorus Chemical Warfare Agents*", in: Hartley, F. R. (Ed.), *The Chemistry of Organophosphorus Compounds*, Vol. *4*, John Wiley & Sons, Chichester, 1996, pp 781−840.

(4) Bajgar, J. *Adv. in Clin. Chem.* **2004**, *38*, 151.

(5) (a) Kuca, K.; Jun, D.; Musilek, K. *Mini-Rev. Med. Chem.* **2006**, *6*, 269. (b) Musilek, K.; Dolezal, M.; Gunn-Moore, F.; Kuca, K. *Med. Res. Rev.* **2011**, *31*, 548.

(6) Abele, E.; Abele, R.; Lukecics, E. *Chem. Heter. Comp* **2003**, *39*, 825.

(7) For comprehensive reviews, see: (a) Chaudhuri, P. *Coord. Chem. Rev.* **2003**, *243*, 143. (b) Milios, C. J.; Stamatatos, Th. C.; Perlepes, S. P. *Polyhedron* **2006**, *25*, 134. (c) Milios, C. J.; Piligkos, S.; Brechin, E. K. *Dalton Trans.* **2008**, 1809. For other relevant papers, see: (d) Stamatatos, Th. C.; Foguet-Albiol, D.; Stoumpos, C. C.; Raptopoulou, C. P.; Terzis, A.; Wernsdorfer, W.; Perlepes, S. P.; Christou, G. *J. Am. Chem. Soc.* **2005**, *127*, 15380. (e) Stamatatos, Th. C.; Foguet-Albiol, D.; Lee, S.- C.; Stoumpos, C. C.; Raptopoulou, C. P.; Terzis, A.; Wernsdorfer, W.; Hill, S. O.; Perlepes, S. P.; Christou, G. *J. Am. Chem. Soc.* **2007**, *129*, 9484. (f) Zaleski, C. M.; Weng, T.- C.; Dendrinou-Samara, C.; Alexiou, M.; Kanakaraki, P.; Hsieh, W.- Y.; Kampf, J.; Penner-Hahn, J. E.; Pecoraro, V. L.; Kessissoglou, D. P. *Inorg. Chem.* **2008**, *47*, 6127. (g) Roubeau, O.; Lecren, L.; Li, Y.- G.; Le Goff, X. F.; Clérac, R. *Inorg. Chem. Commun.* **2005**, *8*, 314. (h) Dendrinou-Samara, C.; Zaleski, C. M.; Evagorou, A.; Kampf, J. W.; Pecoraro, V. L.; Kessissoglou, D. P. *Chem. Commun.* **2003**, 2668. (i) Alexiou, M.; Dendrinou-Samara, C.; Karagianni, A.; Biswas, S.; Zaleski, C. M.; Kampf, J.; Yoder, D.; Penner-Hahn, J. E.; Pecoraro, V. L.; Kessissoglou, D. P. *Inorg. Chem.* **2003**, *42*, 2185. (j) Afrati, T.; Dendrinou-Samara, C.; Raptopoulou, C. P.; Terzis, A.; Tangoulis, V.; Kessissoglou, D. P. *Angew. Chem., Int. Ed.* **2002**, *41*, 2148.

(8) (a) Khanra, S.; Weyhermuller, Th.; Chaudhuri, P. *Dalton Trans.* **2008**, 4885. (b) Stamatatos, Th. C.; Luisi, B. S.; Moulton, B.; Christou, G. *Inorg. Chem.* **2008**, *47*, 1134. (c) Khanra, S.; Weyhermüller, Th.; Chaudhuri, P. *Dalton Trans.* **2007**, 4675. (d) Lampropoulos, C.; Stamatatos, Th. C.; Abboud, K. A.; Christou, G. *Inorg. Chem.* **2009**, *48*, 429. (e) Escuer, A.; Cordero, B.; Solans, X.; Font-Bardia, M.; Calvet, T. *Eur. J. Inorg. Chem.* **2008**, 5082. (f) Escuer, A.; Esteban, J.; Roubeau, O. *Inorg. Chem.* **2011**, *50*, 8893. (g) Escuer, A.; Esteban, J.; Aliaga-Alcalde, N.; Font-Bardia, M.; Calvet, T.; Roubeau, O.; Teat, S. J. *Inorg. Chem.* **2010**, *49*, 2259.

(9) Breslow, R.; Chipman, D. *J. Am. Chem. Soc.* **1965**, *87*, 4195.

(10) Breslow, R.; Overman, L. E. *J. Am. Chem. Soc.* **1970**, *92*, 1075.
(11) Farell, N. P. "*Uses of Inorganic Chemistry in Medicine*", The Royal Society of Chemistry, London, UK, 1999.
(12) (a) Weder, E.; Hambley, T. W.; Kennedy, B. J.; Lay, P. A.; Foran, G. J.; Rich, A. M. *Inorg. Chem.* **2001**, *40*, 1295. (b) Zhou, Q.; Hambley, T. W.; Kennedy, B. J.; Lay, P. A.; Turner, P.; Warwick, B.; Biffin, J. R.; Regtop, H. L. *Inorg. Chem.* **2000**, *39*, 3742.
(13) (a) Wong, E.; Giandomenico, C. M. *Chem. Rev.* **1999**, *99*, 2451. (b) Lippert, B., Ed. *Cisplatin: Chemistry and Biochemistry of a Leading Anticancer Drug*, Wiley-VCH: Weinheim, Germany, 1999. (c) Galanski, M.; Jakupec, M. A.; Keppler, B. K. *Curr. Med. Chem.* **2005**, *12*, 2075.
(14) (a) Jawbry, S.; Freikman, I.; Najajreh, Y.; Manuel Perez, J.; Gibson, D. *J. Inorg. Biochem.* **2005**, *99*, 1983. (b) Eryazici, I.; Moorefield, C. N.; Newkome, G. R. *Chem. Rev.* **2008**, *108*, 1834.
(15) Marzano, C.; Mazzega Sbovata, S.; Gandin, V.; Colavito, D.; Del Giudice, E.; Michelin, R. A.; Venzo, A.; Seraglia, R.; Benetollo, F.; Schiavon, M.; Bertani, R. *J. Med. Chem.* **2010**, *53*, 6210.
(16) Abu-Surrah, A. S.; Kettunen, M. *Curr. Med. Chem.* **2006**, *13*, 1337.
(17) Hambley, T. W. *Science* **2007**, *318*, 1392 and reference cited therein..
(18) Komeda, S.; Casini, A. *Curr. Topics in Med. Chem.* **2012**, *12*, 219.
(19) (a) Muchova, T.; Quintal, S. M.; Farrell, N. P.; Brabec, V.; Kasparkova, J. *J. Biol. Inorg. Chem.* **2012**, *17*, 239. (b) Griffith, D. M.; Duff, B.; Suponitsky, K. Y.; Kavanagh, K.; Morgan, M. P.; Egan, D.; Marmion, C. J. *J. Inorg. Biochem.* **2011**, *105*, 793.
(20) Kontek, R.; Matawska-Wasowska, K.; Kalinowska-Lis., U.; Kontek, B.; Ochocki, J. *Acta Pol. Pharm.* **2011**, *68*, 127.
(21) (a) Caires, A. C. *Anticancer Agents Med. Chem.* **2007**, *7*, 484. (b) Campanella, N. C.; Demartini, M.; Torres, C.; de Almeida, E. T.; Gouvêa, C. M. C. P. *Genetics and Molecular Biology* **2012**, *35*, 159.
(22) Glynn, C. W.; Turnbull, M. M. *Trans. Met. Chem.* **2002**, *27*, 822.
(23) Dimiza, F.; Papadopoulos, A. N.; Tangoulis, V.; Psycharis, V.; Raptopoulou, C. P.; Kessissoglou, D. P.; Psomas, G. *Dalton Trans.* **2010**, *39*, 4517.
(24) Bruker AXS Inc.: Madison, WI, 2003.
(25) *Crystal Clear*, Rigaku/MSC Inc, The Woodlands, Texas, USA, 2005.
(26) (a) Sheldrick, G. M. SHELXS-97, *Structure Solving Program*, University of Göttingén, Germany, 1997. (b) Sheldrick, G. M. SHELXL-97, *Program for the Refinement of Crystal Structures from Diffraction Data*, University of Göttingén, Germany, 1997.
(27) *Mercury*; Bruno, I. J.; Cole, J. C.; Edgington, P. R.; Kessler, M. K.; Macrae, C. F.; McCabe, P.; Pearson, J.; Taylor, R. *Acta Crystallogr., Sect. B* **2002**, *58*, 389.
(28) Bradenburg, K. *DIAMOND, Release 3.1f*, Crystal Impact GbR; Bonn, Germany, 2008.
(29) Lakowicz, J. R. *Principles of Fluorescence Spectroscopy*, 3rd ed., Springer, New York, 2006.
(30) Dimiza, F.; Fountoulaki, S.; Papadopoulos, A. N.; Kontogiorgis, C. A.; Tangoulis, V.; Raptopoulou, C. P.; Psycharis, V.; Terzis, A.; Kessissoglou, D. P.; Psomas, G. *Dalton Trans.* **2011**, *40*, 8555.
(31) For representative reviews, see: (a) Brechin, E. K. *Chem. Commun.* **2005**, 5141. (b) Winpenny, R. E. P. *J. Chem. Soc., Dalton Trans.* **2002**, 1. (c) Bagai, R.; Christou, G. *Chem. Soc. Rev.* **2009**, *38*, 1011. (d) Tasiopoulos, A. J.; Perlepes, S. P. *Dalton Trans.* **2008**, 5537. (e) Stamatatos, Th. C.; Christou, G. *Inorg. Chem.* **2009**, *48*, 3308. (f) Christou, G. *Polyhedron* **2005**, *24*, 2065. (g) Stamatatos, Th. C.; Efthymiou, C. G.; Stoumpos, C. C.; Perlepes, S. P. *Eur. J. Inorg. Chem.* **2009**, 3361.
(32) Hanania, G. I. H.; Irvine, D. H.; Schurauh, F. *J. Chem. Soc.* **1965**, 1149.
(33) (a) Milios, C. J.; Stamatatos, Th. C.; Kyritsis, P.; Terzis, A.; Raptopoulou, C. P.; Vicente, R.; Escuer, A.; Perlepes, S. P. *Eur. J. Inorg. Chem.* **2004**, 2885. (b) Nordquest, K. W.; Phelps, D. W.; Little, W. F.; Hodgson, D. J. *J. Am. Chem. Soc.* **1976**, *98*, 1104.
(34) (a) Papatriantafyllopoulou, C.; Efthymiou, C. G.; Raptopoulou, C. P.; Terzis, A.; Manessi-Zoupa, E.; Perlepes, S. P. *Spectrochim. Acta, Part A* **2008**, *70*, 718. (b) Papatriantafyllopoulou, C.; Stamatatos, Th. C.; Wernsdorfer, W.; Teat, S. J.; Tasiopoulos, A. J.; Escuer, A.; Perlepes, S. P. *Inorg. Chem.* **2010**, *49*, 10486.
(35) (a) Chaudhuri, P.; Winter, M.; Flörke, U.; Houpt, H.- J. *Inorg. Chim. Acta* **1995**, *232*, 125. (b) Papatriantafyllopoulou, C.; Raptopoulou, C. P.; Terzis, A.; Manessi-Zoupa, E.; Perlepes, S. P. *Z. Naturforsch.* **2006**, *61b*, 37. (c) Stamatatos, Th. C.; Escuer, A.; Abboud, K. A.; Raptopoulou, C. P.; Perlepes, S. P.; Christou, G. *Inorg. Chem.* **2008**, *47*, 11825.
(36) (a) Perlepes, S. P.; Garoufis, A.; Sletten, G.; Bakalbassis, E. G.; Plakatouras, G.; Katsarou, E.; Hadjiliadis, N. *Inorg. Chim. Acta* **1997**, *261*, 93. (b) Pratihar, J.; Maiti, N.; Pattanayak, P.; Chattopadhyay, S. *Polyhedron* **2005**, *24*, 1953.
(37) (a) Newkome, G. R.; Fronczek, F. R.; Gupta, V. K.; Puckett, W. E.; Pantaleo, D. C.; Kiefer, G. E. *J. Am. Chem. Soc.* **1982**, *104*, 1782. (b) Anbei, J.; Krüger, C.; Pfeil, B. *Acta Crystallogr., Sect. C* **1987**, *43*, 2334. (c) Fronczek, F. R.; Kahwa, I.; Lu, S.; Newkome, G. R.; Ollino, M. A.; Pitts, W. D.; Sittattrakul, A.; Wang, J. C.; Watkins, S. F. *Acta Crystallogr., Sect. C* **1988**, *44*, 933.
(38) For example, see: (a) Tannai, H.; Koizumi, T.; Tanaka, K. *Inorg. Chim. Acta* **2007**, *360*, 3075. (b) Barrell, M. J.; Leigh, D. A.; Lusby, P. J.; Slawin, A. M. Z. *Angew. Chem., Int. Ed.* **2008**, *47*, 8036. (c) Akinade, K. A.; Adeyemo, A.; Butcher, R. J.; Sinn, E. *J. Crystallogr. Spectr. Res.* **1986**, *16*, 597. (d) Bröring, M.; Kleeberg, C. *Z. Anorg. Allg. Chem.* **2007**, *633*, 2210. (e) Meder, M.; Galka, C. H.; Gade, L. H. *Monatsh. Chem.* **2005**, *136*, 1693.
(39) (a) Milinkovic, S. U.; Parac, T. N.; Djuran, M. I.; Kostic, N. M. *J. Chem. Soc., Dalton Trans.* **1997**, 2771. (b) Pacholska-Dudziak, J.; Skonieczny, J.; Pawlicki, J.; Szterenberg, L.; Ciunic, Z.; Latos-Grazynski, L. *J. Am. Chem. Soc.* **2008**, *130*, 6182. (c) Kamar, K. K.; Das, S.; Hung, C.- H.; Castineiras, A.; Kuzmin, M. D.; Rillo, C.; Bartolome, J.; Goswami, S. *Inorg. Chem.* **2003**, *42*, 5367. (d) Bröring, M.; Kleeberg, C. *Inorg. Chim. Acta* **2009**, *362*, 1065. (e) Hanot, V. P.; Robert, T. D.; Haasnoot, J. G.; Kooijman, H.; Spek, A. L. *J. Chem. Crystallogr.* **1998**, *28*, 343. (f) Mulqi, M.; Stephens, F. S.; Vagg, R. S. *Inorg. Chim. Acta* **1982**, *62*, 221. (g) Zhu, Z.; Kojima, M.; Nakajima, K. *Inorg. Chim. Acta* **2005**, *358*, 476. (h) Mazet, C.; Gade, L. H. *Chem.—Eur. J.* **2003**, *9*, 1759. (i) Siggelkow, B.; Meder, M. B.; Galka, C. H.; Gade, L. H. *Eur. J. Inorg. Chem.* **2004**, 3424. (j) Patra, D.; Pratihar, J.; Shee, B.; Pattanayak, P.; Chattopadhyay, S. *Polyhedron* **2006**, *25*, 2637. (k) Zhang, M.; Inamo, M.; Kojima, M.; Nakajima, K. *Inorg. Chim. Acta* **2007**, *360*, 3040.
(40) (a) Zhang, J.; Wang, X.; Tu, C.; Lin, J.; Ding, J.; Lin, L.; Wang, Z.; He, C.; Yan, C.; You, X.; Guo, Z. *J. Med. Chem.* **2003**, *46*, 3502. (b) Gao, X.; Wang, X.; Ding, J.; Lin, L.; Li, Y.; Guo, Z. *Inorg. Chem. Commun.* **2006**, *9*, 722. (c) Shi, D.; Hambley, T. W.; Freeman, H. C. *J. Inorg. Biochem.* **1999**, *73*, 173. (d) Peters, J. C.; Harkins, S. B.; Brown, S. D.; Day, M. W. *Inorg. Chem.* **2001**, *40*, 5083. (e) Sanz Miguel, P. J.; Roitzsch, M.; Yin, L.; Lax, P. M.; Holland, L.; Krizanovic, O.; Lutterbeck, M.; Schürmann, M.; Fusch, E. C.; Lippert, B. *Dalton Trans.* **2009**, 10774. (f) Chen, J.- L.; Chang, S.- Y.; Chi, Y.; Chen, K.; Cheng, Y.- M.; Lin, C.- W.; Lee, G.- H.; Chou, P.- T.; Wu, C.- H.; Shih, P.- I.; Shu, C.- F. *Chem. Asian. J.* **2008**, *3*, 2112. (g) Castineiras, A.; Garcia-Santos, I.; Saa, M. *Z. Anorg. Allg. Chem.* **2008**, *634*, 2281.
(41) Nieuwenhuis, H. A.; Haasnoot, J. G.; Hage, R.; Reedijk, J.; Snoeck, T. L.; Stufkens, D. J.; Vos, J. G. *Inorg. Chem.* **1991**, *30*, 48 and references cited therein..
(42) (a) Herebian, D.; Bothe, E.; Neese, F.; Weyhermuller, T; Wieghardt, K. *J. Am. Chem. Soc.* **2003**, *125*, 9116. (b) Janzen, D. E.; Van Derveer, D. G.; Mehne, L. F.; da Silva Filho, D. A.; Bredas, J.- L.; Grant, G. J. *Dalton Trans.* **2008**, 1872. (c) Pilia, L.; Espa, D.; Barsella, A.; Fort, A.; Makedonas, C.; Marchio, L.; Mercuri, M. L.; Serpe, A.; Mitsopoulou, C. A.; Deplano, P. *Inorg. Chem.* **2011**, *50*, 10015.
(43) Tan, C.; Liu, J.; Li, H.; Zheng, W.; Shi, S.; Chen, L.; Ji, L. *J. Inorg. Biochem.* **2008**, *102*, 347.
(44) Wang, Y.; Zhang, H.; Zhang, G.; Tao, W.; Tang, S. *J. Lumin.* **2007**, *126*, 211.
(45) Deepa, S.; Mishra, A. K. *J. Pharm. Biomed. Anal.* **2005**, *38*, 556.

(46) (a) Zhang, Q.; Liu, J.; Chao, H.; Xue, G.; Ji, L. *J. Inorg. Biochem.* **2001**, *83*, 49. (b) Turel, I.; Kljun, J. *Curr. Top. Med. Chem.* **2011**, *11*, 2661.
(47) (a) Afrati, T.; Pantazaki, A. A.; Dendrinou-Samara, C.; Raptopoulou, C.; Terzis, A.; Kessissoglou, D. P. *Dalton Trans.* **2010**, *39*, 765. (b) Wirth, S.; Rohbogner, C. J.; Cieslak, M.; Kazmierczak-Baranska, J.; Donevski, S.; Nawrot, B.; Lorenz, I. P. *J. Biol. Inorg. Chem.* **2010**, *15*, 429. (c) Cabeza, J. A.; del Rio, I.; Riera, V.; Suarez, M.; Alvarez-Rua, C.; Garcia-Granda, S.; Chuang, S. H.; Hwu, J. R. *Eur. J. Inorg. Chem.* **2003**, 4159. (d) Surendra Babu, M. S.; Hussain Reddy, K.; Krishna, P. G. *Polyhedron* **2007**, *26*, 572. (e) Chitrapriya, N.; Mahalingam, V.; Zeller, M.; Natarajan, K. *Inorg. Chim. Acta* **2010**, *363*, 3685.
(48) Pyle, A. M.; Rehmann, J. P.; Meshoyrer, R.; Kumar, C. V.; Turro, N. J.; Barton, J. K. *J. Am. Chem. Soc.* **1989**, *111*, 3053.
(49) Long, E. C.; Barton, J. K. *Acc. Chem. Res.* **1990**, *23*, 271.
(50) (a) Li, D.; Tian, J.; Gu, W.; Liu, X.; Yan, S. *J. Inorg. Biochem.* **2010**, *104*, 171. (b) Liu, J.; Zhang, H.; Chen, C.; Deng, H.; Lu, T.; Li, L. *Dalton Trans.* **2003**, 114. (c) Garcia-Gimenez, J. L.; Alzuet, G.; Gonzalez-Alvarez, M.; Liu-Gonzalez, M.; Castineiras, A.; Borras, J. *J. Inorg. Biochem.* **2009**, *103*, 243.
(51) Wilson, W. D.; Ratmeyer, L.; Zhao, M.; Strekowski, L.; Boykin, D. *Biochemistry* **1993**, *32*, 4098.
(52) Zhao, G.; Lin, H.; Zhu, S.; Sun, H.; Chen, Y. *J. Inorg. Biochem.* **1998**, *70*, 219.
(53) Pasternack, R. F.; Cacca, M.; Keogh, B.; Stephenson, T. A.; Williams, A. P.; Gibbs, F. J. *J. Am. Chem. Soc.* **1991**, *113*, 6835.
(54) Dimiza, F.; Perdih, F.; Tangoulis, V.; Turel, I.; Kessissoglou, D. P.; Psomas, G. *J. Inorg. Biochem.* **2011**, *105*, 476.
(55) Rajendiran, V.; Karthik, R.; Palaniandavar, M.; Stoeckli-Evans, H.; Periasamy, V. S.; Akbarsha, M. A.; Srinag, B. S.; Krishnamurthy, H. *Inorg. Chem.* **2007**, *46*, 8208.
(56) (a) Laitinen, O. H.; Hytonen, V. P.; Nordlund, H. R.; Kulomaa, M. S. *Cell. Mol. Life Sci.* **2006**, *63*, 2992. (b) Tarushi, A.; Totta, X.; Raptopoulou, C. P.; Psycharis, V.; Psomas, G.; Kessissoglou, D. P. *Dalton Trans.* **2012**, *41*, 7082.
(57) Song, Y.; Wu, Q.; Yang, P.; Luan, N.; Wang, L.; Liu, Y. *J. Inorg. Biochem.* **2006**, *100*, 1685.
(58) Pratviel, G.; Bernadou, J.; Meunier, B. *Adv. Inorg. Chem.* **1998**, *45*, 251.
(59) Jancso, A.; Nagy, L.; Moldrheim, E.; Sletten, E. *J. Chem. Soc., Dalton Trans.* **1999**, 1587.
(60) (a) Psomas, G. *J. Inorg. Biochem.* **2008**, *102*, 1798. (b) Skyrianou, K. C.; Perdih, F.; Papadopoulos, A. N.; Turel, I.; Kessissoglou, D. P.; Psomas, G. *J. Inorg. Biochem.* **2011**, *105*, 1273. (c) Tarushi, A.; Polatoglou, E.; Kljun, J.; Turel, I.; Psomas, G.; Kessissoglou, D. P. *Dalton Trans.* **2011**, *40*, 9461.
(61) Dimitrakopoulou, A.; Dendrinou-Samara, C.; Pantazaki, A. A.; Alexiou, M.; Nordlander, E.; Kessissoglou, D. P. *J. Inorg. Biochem.* **2008**, *102*, 618.
(62) (a) Senapoti, S.; Jasimuddin, S.; Mostafa, G.; Lu, T. -H.; Sinha, C. *Polyhedron* **2006**, *25*, 1571. (b) Panda, M.; Das, S.; Mostafa, G.; Castineiras, A.; Goswami, S. *Dalton Trans.* **2005**, 1249.
(63) Shimazaki, Y.; Yajima, T.; Tani, F.; Karasawa, S.; Fukui, K.; Naruta, Y.; Yamauchi, O. *J. Am. Chem. Soc.* **2007**, *129*, 2559.
(64) Carter, M. T.; Rodriguez, M.; Bard, A. J. *J. Am. Chem. Soc.* **1989**, *111*, 8901.
(65) (a) Dimiza, F.; Papadopoulos, A. N.; Tangoulis, V.; Psycharis, V.; Raptopoulou, C. P.; Kessissoglou, D. P.; Psomas, G. *J. Inorg. Biochem.* **2012**, *107*, 54. (b) Tsiliou, S.; Kefala, L.- A.; Perdih, F.; Turel, I.; Kessissoglou, D. P.; Psomas, G. *Eur. J. Med. Chem.* **2012**, *48*, 132.
(66) Tabassum, S.; Parveen, S.; Arjmand, F. *Acta Biomaterialia* **2005**, *1*, 677.